

Local structure determination of NH₂ on Si(111)-(7×7)S. Bengió,¹ H. Ascolani,¹ N. Franco,³ J. Avila,² M. C. Asensio,^{2,3} A. M. Bradshaw,⁴ and D. P. Woodruff^{4,5}¹CONICET and Centro Atómico Bariloche, Comisión Nacional de Energía Atómica, 8400 Bariloche, Argentina²Instituto de Ciencia de Materiales, CSIC, Cantoblanco, 28049 Madrid, Spain³LURE, Bât. 209D, Université Paris-Sud, F91405 Orsay, France⁴Fritz-Haber-Institut der Max-Planck-Gesellschaft, Faradayweg 4-6, 14195 Berlin, Germany⁵Physics Department, University of Warwick, Coventry CV4 7AL, United Kingdom

(Received 6 October 2003; revised manuscript received 13 January 2004; published 30 March 2004)

N 1s scanned-energy mode photoelectron diffraction has been used to determine the local adsorption geometry of adsorbed NH₂ species on Si(111)(7×7) resulting from reaction with NH₃ at room temperature. The results show that NH₂ is adsorbed (almost) exclusively atop Si surface rest atoms with a Si-N bond length of 1.71 ± 0.02 Å and very little modification of the geometry of the Si atoms in the layer below. Any coadsorbed NH on the surface is either of low relative coverage or is also adsorbed in local atop sites. There is evidence that a small fraction ($8 \pm 7\%$) of the NH_x species may occupy sites atop Si surface adatoms.

DOI: 10.1103/PhysRevB.69.125340

PACS number(s): 68.43.-h, 82.45.Jn, 61.14.Qp

I. INTRODUCTION

The interaction of ammonia with Si surfaces has attracted quite a lot of attention in the last 10–15 years, motivated in part by the interest in silicon nitride and the potential utility of this material in microelectronics. For the purposes of surface nitridation relatively high sample temperatures are used, but in an attempt to gain a clearer understanding of the underlying surface chemistry, lower temperature investigations have also been conducted. In particular, the initial stages of the reaction of ammonia with the reconstructed clean Si(111)(7×7) surface have been investigated by using a range of different experimental techniques including ultraviolet photoelectron spectroscopy (UPS),¹ high-resolution electron energy loss spectroscopy (HREELS),^{2,3,4} core level photoelectron spectroscopy using conventional x-ray sources,^{5,6} and soft x-ray synchrotron radiation (SXPS),^{7,8} scanning tunneling microscopy (STM),⁹ Auger electron spectroscopy (AES),¹⁰ and temperature programmed desorption.^{3,4} There was an early consensus that at room temperature NH₃ dissociates to coadsorbed amino (NH₂) and atomic hydrogen, and indeed this reaction appears to occur even at 100 K. At much higher temperatures complete dissociation occurs, leading to atomic nitrogen being left on (or in) the surface. More recent HREELS investigations,^{3,4} however, have found evidence for both adsorbed NH₂ and coadsorbed NH, even at room temperature, and over a range of surface coverage. High resolution SXPS studies of the N 1s emission after room temperature adsorption have also identified two principal states with a photoelectron binding energy difference of approximately 0.8 eV which have been attributed to these NH₂ and NH species.⁸

Studies of the interaction of NH₃ with the reconstructed Si(100)(2×1) surface have also shown clear evidence of dissociation to coadsorbed NH₂ and H at room temperature, although on this surface there is no evidence of further dissociation at this relatively low temperature. A quantitative structure determination^{11,12} by scanned-energy mode photoelectron diffraction (PhD) (Ref. 13) found that the NH₂ species bonds to one end of the Si surface dimers of this surface

such that the N atom occupies an off-atop site with a Si-N bond length of 1.73 ± 0.03 Å and a tilt of this bond relative to the surface normal of $21 \pm 4^\circ$. It is generally believed that on Si(100) the H atom removed from the dissociating NH₃ is bonded to the Si atom at the other end of the surface dimer, and indeed that it is the interaction of the incoming NH₃ species with the two dangling bonds at either end of a Si surface dimer which enables the dissociation, a view supported by theoretical calculations.¹⁴

In the case of the Si(111)(7×7) surface, the only structural information concerning the adsorption geometry of the adsorbed NH_x species is largely based on speculation. In particular, it has generally been assumed that both NH₂ and H resulting from the initial dissociation must adopt singly coordinated atop sites [similar to the behavior on Si(100)×(2×1)], while the NH species should adopt a twofold coordinated bridging site requiring a local modification of the underlying Si surface structure. Of course, the structure of the Si(111)(7×7) surface is significantly more complicated than that of the Si(100)(2×1) surface which simply comprises pairing of atoms of the bulk-terminated structure (each having two dangling bonds) to produce surface dimers of Si atoms having only one dangling bond each. There is a broad consensus that the structure of the Si(111)(7×7) surface is the dimer-atom-stacking fault (DAS) model first proposed by Takayanagi *et al.*¹⁵ on the basis of high energy electron diffraction data. This structure is shown schematically in Fig. 1. As implied by the name, there are three key ingredients in the reconstruction which serve to reduce the number of Si surface dangling bonds (which would, for a bulk-terminated structure, be one per surface atom and thus 49 dangling bonds per unreconstructed 7×7 surface unit mesh). The formation of surface dimers by pairing of nearest neighbor Si surface atoms that lie along the boundaries of the two halves of the 7×7 unit mesh removes all the dangling bonds of these atoms. The addition of Si adatoms (*A* in Fig. 4) bonded to groups of three surface Si atoms (labeled 1 in Fig. 4 and hereafter referred to as Si₁) reduces the number of dangling bonds in these groups from three (one per surface Si₁ atom below the adatom) to one (at the adatom). In addi-

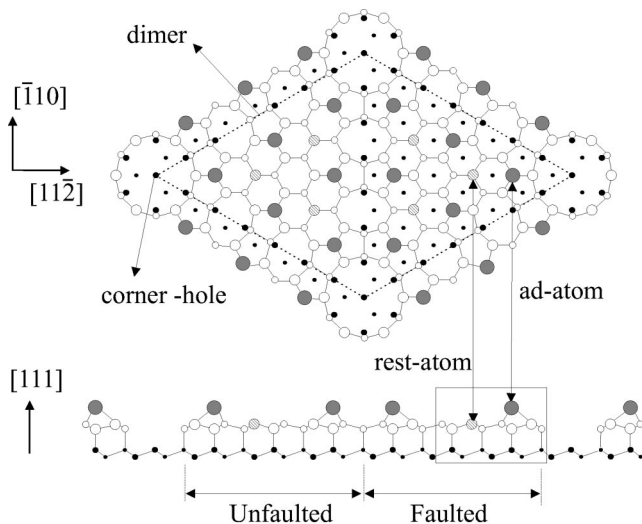


FIG. 1. Schematic diagram of the dimer-adatom-stacking fault (DAS) model of the Si(111)(7 \times 7) surface. A rest-atom/adatom pair such as that implicated in the $\text{NH}_3 \rightarrow \text{NH}_2 + \text{H}$ dissociation is highlighted in the superimposed rectangle.

tion, a stacking fault between the substrate and the outermost double layer of the surface in one half of the surface unit mesh assists in the organization of these structural elements. This reconstructed surface has in a single surface unit mesh 12 adatoms, each with a dangling bond perpendicular to the surface, and six so-called rest atoms (R in Fig. 4) which are outer layer Si atoms (nominally in the same layer as the Si_1 atoms) of the original surface double layer which retain the original local bonding of the bulk-terminated structure and thus also retain a single dangling bond perpendicular to the surface. The DAS reconstruction thus reduces the number of dangling bonds of the bulk-terminated structure from 49 per surface unit mesh to 19 (including one “corner hole” site—see Fig. 1).

This surface therefore has two distinctly different types of dangling-bond sites for singly coordinated NH_2 adsorption, atop either adatoms or rest atoms. Notice that there are subtle differences in the adatom and rest atom sites in the two inequivalent halves of the surface unit mesh (due to the stacking fault), and between the surroundings of adatom sites near the center or the edge of the unit mesh shown in Fig. 1. As on the Si(100) surface, theoretical calculations indicate that on Si(111)(7 \times 7) the dissociation of NH_3 (Ref. 16) [and H_2 (Ref. 17)] proceeds through interaction with two adjacent surface dangling bonds onto which the dissociated products adsorb; adjacent pairs of such sites involve both a rest atom and an adatom (see the rectangular frame of Fig. 1), so both dangling bond sites are implicated in the reaction. In the case of the NH adsorbate, it has been proposed that this bonds to a twofold coordinated site on the surface by insertion into the backbond of a Si adatom to one its underlying Si neighbors. This picture of the local structure after the initial dissociation has been supported by the results¹⁸ of recent total energy calculations using the extended Hückel theory; these calculations also show very similar adsorption energies for both NH_2 and H at the different adatom and rest atom sites in the surface unit mesh, although the adatom sites do appear to be

avored. It has been argued that the NH_2 species should bond to the Si surface atoms which are initially most depleted of electronic charge, an argument also favoring the adatom site over the rest atom site.¹⁶ Some limited structural information is provided by the results of the STM investigation of the Si(111)(7 \times 7)/ NH_3 surface interaction. In particular, by using atomic-scale resolution images recorded at different bias voltages, and performing scanning tunneling spectroscopy, Avouris and Wolkow⁹ were able to establish at which surface sites the largest changes occurred as a result of the interaction, presumably identifying the reaction sites. This study led to the conclusion that the rest atoms were more reactive than the adatoms, and that of the adatom sites those at the center of the reconstructed unit mesh shown in Fig. 1 were more reactive than those at the corners. However, this investigation did not allow a reliable distinction to be drawn regarding the chemical identity (NH_2 or H) of the species adsorbed at the different sites.

In this paper we present the results of a quantitative surface structure determination of the local adsorption geometry of adsorbed NH_x on Si(111)(7 \times 7), produced by interaction with NH_3 at room temperature, using N 1s PhD. Our results clearly favor occupation of sites atop the rest atoms by NH_2 .

II. EXPERIMENTAL DETAILS

The experiments were carried out at the BESSY I synchrotron radiation facility in Berlin using the HE-TGM 1 beam line.¹⁹ The surface science end-station chamber was equipped with the usual sample handling and surface characterization facilities and a concentric spherical-sector electron spectrometer (VG Scientific, 152 mm radius, three channeltron detection) for recording SXPS data (including those used in the photoelectron diffraction measurements). The Si(111) p -doped samples were degassed for several hours at 900 K using resistive heating, and were then flashed at 1500 K. SXPS and low-energy electron diffraction (LEED) indicated that a clean and well-ordered 7 \times 7 reconstructed surface was obtained following this procedure. The surface was then exposed to 1×10^{-6} mbar s of ammonia at room temperature. Some estimate of the surface coverage may be obtained by comparing the intensity of the N 1s photoemission peak measured on the reacted 7 \times 7 surface with that of the corresponding spectrum taken from a saturated Si(100)(2 \times 1)- NH_2 surface^{11,12} (with an assumed coverage of 0.5 ML). If these two signals are referenced to the intensity of the Si L_{VV} Auger electron emission around 90 eV we obtain an estimated nitrogen coverage on our Si(111)(7 \times 7) surface of 0.13 ML (which would correspond to six N atoms per 7 \times 7 unit mesh). Referencing the N 1s emission intensity to that of the Si 2p photoemission (at a kinetic energy of around 650 eV) led, however, to a much higher coverage estimate of 0.35 ML. It is probable that it is this latter estimate which is in error due to the effects of forward scattering X-ray photoelectron diffraction (XPD) from the Si substrate in these two different surfaces, but the discrepancy means that the more probable value of 0.13 ML must be treated with caution.

A characteristic feature of the HE-TGM beam line which

has proved extremely valuable in PhD determinations of adsorbate structures is the high output flux, but this is achieved in part at the expense of spectral resolution. The general methodology we have applied in these investigations¹³ has therefore been to sacrifice resolution for intensity. In light of a more recent SXPS investigation⁸ of the Si(111)/NH₃ interaction, however, it would have been advantageous to have been able to collect data with a spectral resolution sufficient to identify the N 1s components attributed to coadsorbed NH₂ and NH species, separated by approximately 0.8 eV, but in our low resolution spectra (a full width at half maximum around 3–5 eV across the photon energy range measured) this did not prove possible.

Photoelectron diffraction data using the N 1s photoemission peak were recorded from this Si(111)(7×7)/NH₃ surface in the kinetic energy range 35–445 eV at polar emission angles of 5°, 10°, 15°, 20°, and 30° in the [11 $\bar{2}$], [$\bar{1}\bar{1}$ 2], and [1 $\bar{1}$ 0] high symmetry azimuths at room temperature (see Fig. 1). For each emission direction individual photoelectron energy distribution curves (EDCs) were recorded in a 30-eV range centered on the N 1s emission peak at a succession of photon energies (in 2-eV increments) to cover the necessary kinetic energy range. Each of these EDCs was fitted by a sum of a Gaussian peak with its associated background step and a suitable underlying background, and the resulting peak areas as a function of photoelectron energy were normalized to a smooth spline through the data to give individual photoelectron diffraction modulation spectra. Notice that careful generation of the background from the “tails” of the individual EDCs allowed the Si *LMM* and N *KLL* Auger electron peaks at 92 and 380 eV to be subtracted in those spectra in which the N 1s emission overlapped these features.

The PhD modulation spectra resulting from this data reduction process form the basis of the subsequent structure determination described in Sec. III. The oscillations of these modulation curves were found to attenuate strongly with increasing polar emission angle and were comparable to the amplitude of the noise for angles greater than 20°. For this reason, of the complete set of 16 PhD spectra collected in the experiment, only the nine which show the most intense oscillations (e.g., Fig. 3) have been used to determine the surface structure.

III. DATA ANALYSIS AND STRUCTURE DETERMINATION

A full quantitative structure determination from PhD data is based on comparison of the experimental data with the results of computational simulations which take proper account of the effects of multiple elastic electron scattering. However, valuable insight into the correct structural model can often be obtained through the use of methods of direct inversion of the experimental spectra to produce a real-space “image” of the structure, and our standard methodology is based on the integrated use of both methods.²⁰ All such inversion procedures are based on simplifications which are not strictly valid, but they can still provide valuable first indications of the probable adsorption site. In the present case we have used variations of the so-called “projection method”^{21,22} of direct data inversion. This method is based

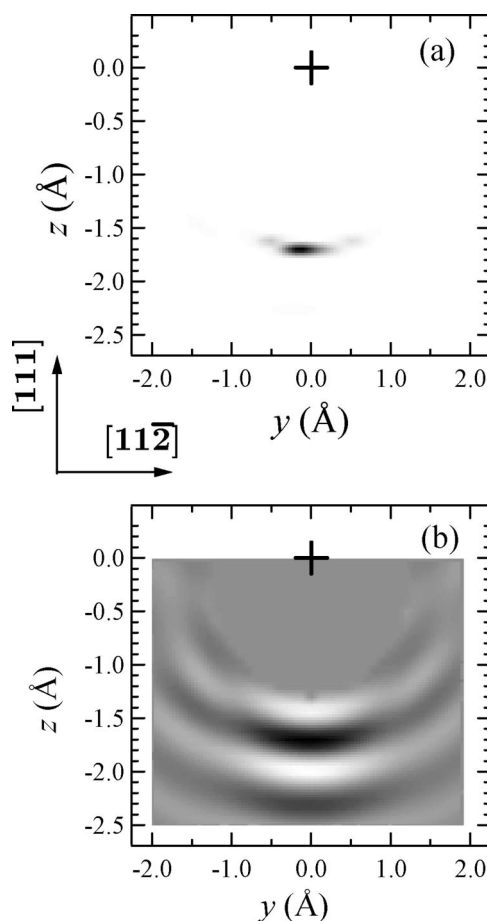


FIG. 2. Results of the application of the projection method, and a variant of it, to obtain a direct inversion of the experimental PhD data (see Figs. 3, 5, or 6). The panels show a gray-scale mapping of a parameter which should take its maximum value in locations in space most likely to correspond to the location of near-neighbor Si backscatterer atoms. Each panel shows a cut perpendicular to the surface passing through the N emitter atom located at (0,0,0). The upper panel (a) uses the standard projection method (Refs. 21 and 22). The lower panel (b) is based on a modified form described elsewhere (Refs. 24 and 25).

on the fact that if the emission direction is aligned with the inter-nuclear axis between the emitter atom and one of its substrate nearest neighbors such that the scattering is through 180°, the PhD modulations are commonly (but not invariably²³) dominated by the interference between the directly emitted component of the photoelectron wavefield and the single-scattering wave generated by the backscattering at this nearest neighbor. A simple projection integral of the experimental PhD spectra onto single-scattering modulation functions calculated over a grid of test sites for a nearest-neighbor backscatterer may therefore be expected to peak near the location corresponding to such a real atom.

Figure 2(a) shows the result of applying this standard projection method to the present data set in the form of a gray-scale mapping in a plane perpendicular to the surface in the [11 $\bar{2}$] azimuth passing through the N emitter atom located at the origin, (0,0,0). A single strong feature is seen approximately 1.7 Å directly below the emitter, strongly suggesting

that the N atoms are atop (or near atop) a surface Si atom. Figure 2(b) shows the results of applying an alternative version of the projection method;^{24,25} the dominant feature, the region of maximum (darkest) intensity is seen to be centered on the same position.

The main conclusions from this first-order structure evaluation is thus that the N emitters are exclusively or partially located in near atop sites. A more detailed structure determination, however, including an accurate determination of the Si-N bond length necessitate a proper simulation of the experimental PhD spectra for different structural models. This procedure may also be expected to help distinguish between adsorption in near atop sites above rest atoms and adatoms, because although the nearest-neighbor scattering geometry is the same, the relative positions of more distant scatterers around these sites is different. The necessary multiple scattering calculations were performed using computational codes developed by Fritzsche, which use an expansion of the scattering processes into scattering paths.^{26,27} The successive scattering events on a scattering path are treated within a Green's function formalism using a magnetic quantum number expansion for the free electron propagator.²⁸ In order to provide an objective measure of the quality of agreement between the simulated and experimental modulation functions it is important to make use of an objective criterion provided by a minimization of a reliability factor (*R* factor). One such *R* factor previously used extensively in PhD structure determinations is R_m ,²⁹ which is a normalized sum of the squares of the differences between experimental and theoretical PhD modulation amplitudes at each data point *i* in the complete set of PhD spectra to be compared:

$$R_m = \sum_i \frac{[\chi_{\text{expt}}(i) - \chi_{\text{theor}}(i)]^2}{[\chi_{\text{expt}}(i)^2 + \chi_{\text{theor}}(i)^2]}.$$

The normalization is such that R_m is equal to zero for a complete agreement between theory and experiment, to unity for no correlation between theory and experiment, and a value of 2 for anticorrelation. In the present study we have also used a second *R* factor R_p in which all the χ values in the above expression are replaced by energy derivatives χ' ; the basis of this alternative has been discussed elsewhere.^{30,25}

To optimize the efficiency of the search of the structural multiparameter space around trial models to find the structure corresponding to the best agreement we use an adapted Newton-Gauss-algorithm.²⁶ In order to define the precision of the final structural parameters, and to establish the formal significance of changes in the *R* factor between different structural models, we use a variance in the minimum value of the *R* factor, R_{min} , defined in a similar fashion to that used in conjunction with the Pendry *R* factor in LEED.³¹ In particular, we take $\text{var}(R_{\text{min}}) = \sqrt{(2/N)}R_{\text{min}}$ where *N* is the number of independent pieces of structural information contained in the data as described by us in more detail elsewhere.³² Any structure which is found to have an associated *R*-factor less than $[R_{\text{min}} + \text{var}(R_{\text{min}})]$ is regarded as acceptable.

An important prerequisite to an effective use of the PhD methodology is a reasonable knowledge of the structure of the underlying substrate onto which the emitter atom is ad-

sorbed (in this case as part of a molecular species). On a typical metal surface it is usually adequate to start the structural optimization by assuming that the substrate has a bulk-terminated structure, and one may then explore the extent to which subtle near-surface distortions influence the data and improve the fit to experiment. In the case of metal surfaces which are significantly reconstructed (commonly as a result of the presence of the adsorbate) various models of the reconstruction and its associated positional parameters may be explored, but such reconstructions usually involve significant atomic displacements in no more than the outermost one or two atomic layers. The modulations seen in PhD are generally dominated by very near-neighbor scatterers, so the results are not very sensitive to assumptions about subtle aspects of the subsurface layer geometries. Indeed, in the present case the fact that the N atoms of the adsorbed species appear to be in atop sites relative to outermost layer Si atoms means that the relatively strong PhD modulations are likely to be dominated by the scattering from this single near-neighbor atom in the favored 180° scattering geometry. This is borne out by the results of multiple scattering simulations which include only this one Si substrate atom and, after an optimization of the geometry (corresponding to a Si-N bond length of 1.70 Å), leads to a good description of the main features of the experimental PhD data, as shown in Fig. 3. The *R* factors for this fit ($R_m = 0.16$, $R_p = 0.28$) are quite low, reflecting the generally good fit. Of course, it is important to conduct calculations on a properly converged cluster of Si atoms to represent the surface structure, but this figure does highlight the highly local character of the structural information of PhD, and shows that an exact description of the substrate structure, and particularly of the location of Si substrate atoms in deeper subsurface layers, is not important. On the other hand, there is some detailed fine structure in the experimental PhD spectra not reproduced by these single-atom substrate scattering calculations, and we may anticipate that these details provide the basis for a more complete site and local geometry determination.

In order to perform these calculations, our starting point has been to assume that the Si(111)(7×7) surface on which the NH₂ species are adsorbed can be described by the structure obtained in a symmetrized dynamical LEED study of the clean surface.³³ Starting from this substrate structure we have explored the optimized positions of the N emitters at different adsorption sites and, in a second stage of optimization, have then adjusted the positions of the near-neighbor Si atoms and the relative position of the underlying bulk. Bearing in mind that the results of both the direct projection method and the simple simulation based on only a single Si substrate atom indicate that the N emitter atoms are essentially atop a surface Si atoms, there are really only two distinct possible sites on the Si(111)(7×7) surface: atop a rest atom, or atop an adatom. Figure 4 shows these two local geometries and the structural parameters which were optimized in attempts to fit the results of the multiple scattering calculations to the experimental PhD spectra. Notice that in the PhD technique the important structural parameters are the locations of scatterer atoms relative to the emitter. Thus while the locations of the Si₂ atoms (labeled 2 in Fig. 4)

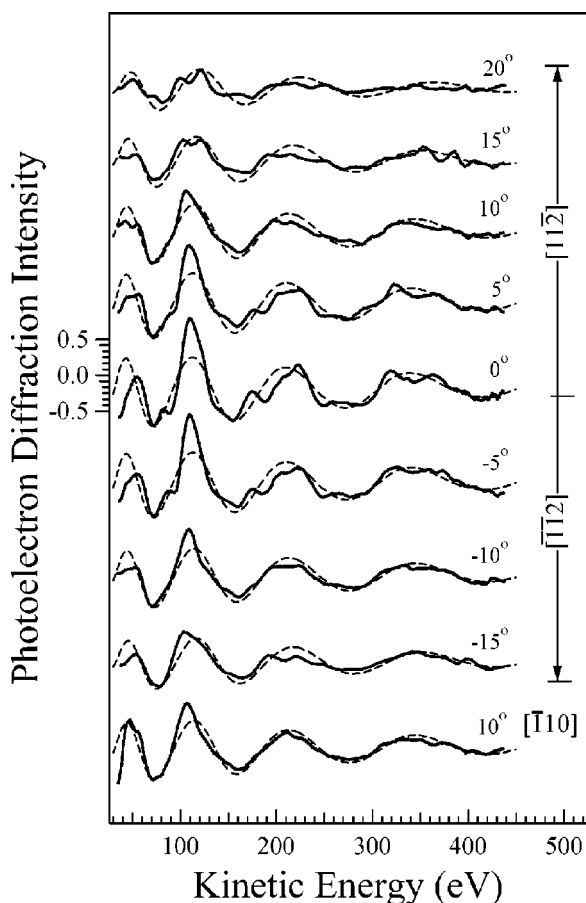


FIG. 3. Comparison of the experimental N 1s PhD spectra (bold lines) from the Si(111)(7×7)/NH₃ surface recorded at different polar emission angles (as noted) and in three different azimuths, with the results of calculations (dashed lines) in which the Si substrate is represented by only a single nearest-neighbor Si atom in an optimized atop geometry with a Si-N distance of 1.70 Å.

which are nearest neighbors to the rest atom (for adsorption atop a rest atom) or the locations of the Si₁ atoms adjacent to the adatom (for adsorption atop an adatom) were varied, the other structural parameter z_{N3} effectively defines the layer spacing of the N atom relative to the rest of the “ideal” rigid Si(111)(7×7) surface. The influence of the relative positions of the near-neighbor Si atoms parallel to the surface was explored by varying the parameter r_1 (Fig. 4) assuming the local threefold symmetry is retained. The possibility that the N atom is not exactly atop the nearest-neighbor Si atoms was also explored, the offset being defined by a Si-N bond tilt angle; as the optimum value of this tilt was found to be zero, the tilt azimuth is irrelevant. Notice too that because of the large 7×7 unit mesh, the various adatom and rest atoms within the unit mesh are not formally equivalent to each other, so in principle the local structural parameters could be different for all the symmetrically inequivalent atoms. We have however, applied the constraint that all adatoms are locally equivalent with regard to these parameters; the same constraint was applied to all rest atoms. One variation of this constraint was to allow Si atoms in the faulted and unfaulted

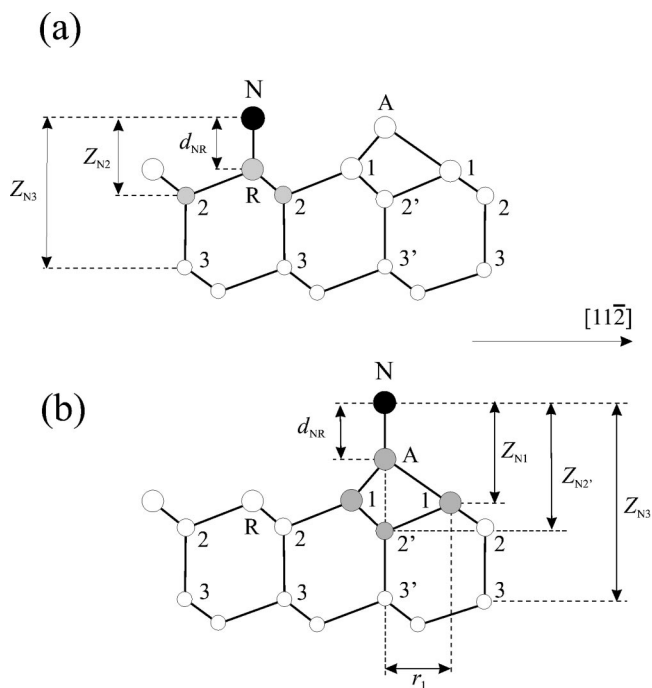


FIG. 4. Schematic side view of the local geometry of the N emitter atom of the adsorbate on the rest atom (R) and adatom (A) sites showing the associated optimized structural parameters.

halves of the surface unit mesh to differ, and we will comment on the effects of this below.

In addition to the structural parameters defining the relative positions of atoms, the vibrational amplitudes of the atoms can also influence the calculated spectra and thus the degree of agreement with experiment. For the substrate Si atoms, of course, the appropriate vibrational amplitudes can be calculated from the published Debye temperature (giving a mean-square vibrational amplitude at room temperature of 0.0037 \AA^2). On the other hand, the vibrational amplitude of the N emitter atoms is not known, and we may expect those of the surface layer(s) of Si atoms to be somewhat larger than those of the underlying bulk. A further complication arises because PhD is sensitive not to the absolute vibrational amplitudes, but to the vibrational amplitudes of the scatterer atoms *relative to the emitter*. For uncorrelated vibrations, one can obtain the square of the relative vibrational amplitude by simply summing the square of the emitter and scatterer vibrations, but for near neighbors, the true figure may be significantly lower due to vibrational correlation. Typically, for nearest neighbors, this can lead to a reduction of about a factor of between 2 and 3. This effect probably contributes to the general observation that, especially at the favored 180° scattering angle, the nearest-neighbor scattering commonly dominates the observed PhD modulations. While some tests were performed on the influence of the vibrational amplitudes in the calculated PhD spectra, the final calculations were all performed with values judged to be reasonably consistent with expectations. In effect this involved assuming that the N vibrational amplitudes were the same as those of the bulk Si atoms, while the nearest-neighbor correlation was assumed to reduce the relative mean square amplitude by a

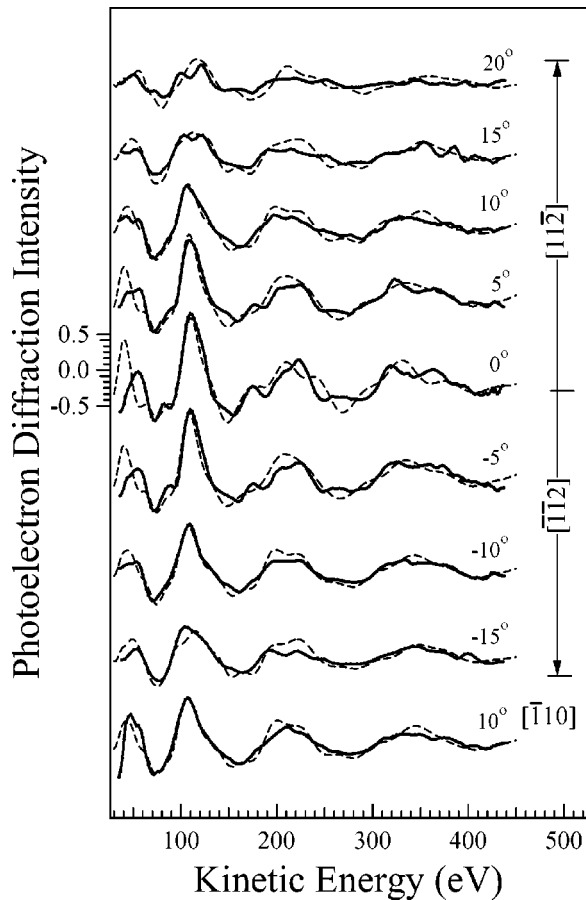


FIG. 5. Comparison of the experimental N 1s PhD spectra (bold lines) from the Si(111)(7×7)/NH₃ surface recorded at different polar emission angles (as noted) and in three different azimuths, with the results of calculations (dashed lines) for the full calculations for the best-fit adsorption geometry with adsorption atop the rest atoms. The associated structural parameter values are listed in Tables I and II.

factor of 2.5. Thus, the relative mean-square vibrational amplitudes of the emitter and bulk Si atoms were set to 0.005 Å² while those of the emitter relative to the nearest-neighbor Si atoms were set to 0.002 Å². The calculated *R* factors are not very sensitive to these parameters, with 50% variations falling well within the variance.

With these constraints applied and the variable structural parameters optimized, the best fit calculations result in the spectra shown in Figs. 5 and 6 for adsorption atop rest atoms and adatoms, respectively. Notice that to obtain these spectra calculations were performed separately for each of the symmetrically inequivalent rest atom or adatom sites with the same local parameters and then the resulting intensities added. For adsorption on the rest atom sites the *R* factor values of *R_m* and *R_p* were 0.12 and 0.22 respectively; the equivalent values for the adatoms sites were 0.18 and 0.42. Visual inspection shows the origin of the different *R*-factor values for the two sites rather clearly. Both calculations yield spectra with additional fine structure, relative to the single atom calculations of Fig. 3, but while those for the rest atoms sites broadly reproduce the fine structure of the experimental

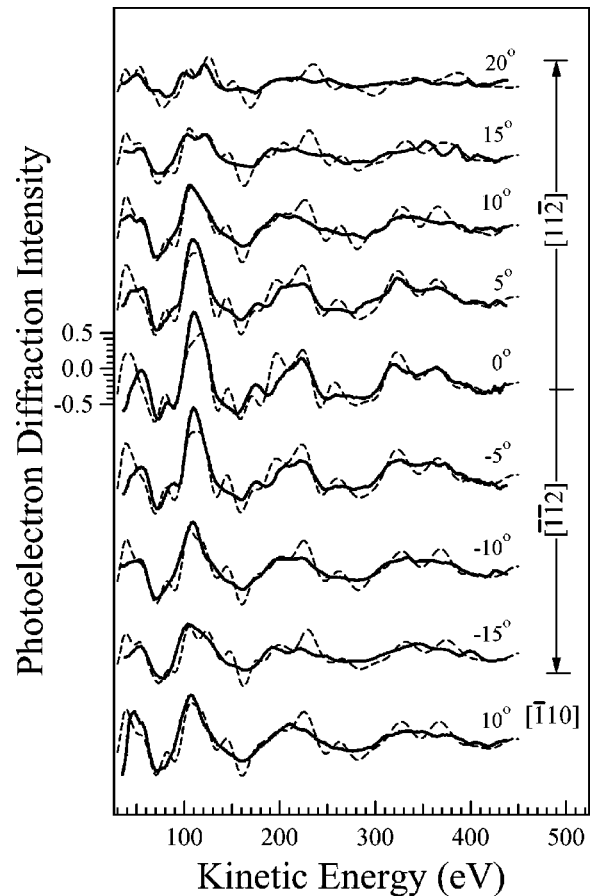


FIG. 6. Comparison of the experimental N 1s PhD spectra (bold lines) from the Si(111)(7×7)/NH₃ surface recorded at different polar emission angles (as noted) and in three different azimuths, with the results of calculations (dashed lines) for the full calculations for the (constrained) best-fit adsorption geometry with adsorption atop the adatom. The associated structural parameter values are listed in Tables II and III.

data, those for the adatom sites are much more intense than these extra features in the experimental data, a fact reflected by the very significantly larger values of the *R* factors. Indeed, as indicated by visual inspection, the optimized geometry of the full cluster calculation for the rest atom site gives a significant improvement in the quality of the fit relative to the calculation which only included the nearest-neighbor Si scatterer, whereas the equivalent calculation for the adatom site actually leads to a reduction in the quality of the fit.

The structural parameter values for the best fit rest atom adsorption geometry are listed in Table I, while the local displacements of the Si atoms perpendicular to the surface, relative to the starting values for the clean Si(111)(7×7) surface, are given in Table II. Notice that for the rest atom adsorption site, allowing the local structure around the adsorbate in the faulted and unfaulted halves of the surface unit mesh to differ did not lead to a difference in the structure. Within this structure the Si atom movements induced by the adsorption appear to be very small (and not formally significant). By contrast, the equivalent optimized parameter values of the adatom adsorption site structure, with the local geometry in the two halves of the unit mesh constrained to be the

TABLE I. Optimum values of the structural parameters determined by photoelectron diffraction for a Si(111)(7×7) surface with NH_x fragments adsorbed atop the silicon rest atoms.

	Unfaulted half	Faulted half
d_{NR} (Å)	1.71±0.02	
θ_{NR} (°)	0±8	
z_{N2} (Å)	2.38±0.12	2.38±0.12
z_{N3} (Å)	4.80±0.08	4.80±0.08

same (Tables II and III), do show quite significant movements of the outermost Si atoms. For the adatom adsorption site, a significant improvement in the R factors (to $R_m=0.14$ and $R_p=0.24$) could be achieved by allowing the local structure in the two halves of the unit mesh to differ, but this does lead to some significant structural distortion (Table IV). In particular, the Si(2') atom spacing differs by 0.18 Å in the two halves of the unit mesh (also leading to an increase in $z_{\text{N3}'}$). While this fit is just at the limits of the variance of the best-fit restatom adsorption site geometry, the need to introduce additional (and probably unphysical) structural parameter variations causes us to reject this solution.

Of course, the fact that the calculated PhD spectra for the best-fit adatom site geometry shows much too fine a structure, and gives a worse fit than the calculation for the near-neighbor scattering alone, indicates that a better fit could be achieved by enhancing the relative vibrational amplitudes of the bulk Si atoms to suppress the importance of these scatterers involving longer scattering paths and thus shorter periodicity modulations. This is, indeed, the case. A much better fit ($R_m=0.14$, $R_p=0.22$) can be achieved by retaining the relative mean-square vibrational amplitude of the emitter and the nearest-neighbor Si atoms at 0.002 Å² but increasing that relative to the bulk Si atoms to 0.020 Å². Clearly, however, such a solution is unphysical—the implied root mean square vibrational amplitude of the N atom is very large (0.14 Å),

TABLE II. Displacements perpendicular to the surface of the near-surface silicon atoms determined by photoelectron diffraction in this study from the reacted Si(111)(7×7)/NH₂ surface relative to their starting positions in the clean Si(111)(7×7) as determined by LEED. As in Table III, in the case of adsorption atop silicon adatoms the solution was obtained with the constraint that the structural parameters in the faulted and unfaulted halves of the surface unit mesh should be the same. In this case, the perpendicular displacements are measured with respect to the positions in the unfaulted part of the clean 7×7 surface unit mesh.

Rest-atom site	Unfaulted half	Faulted half
	Δz_{R} (Å)	0.03±0.08
Δz_2 (Å)	0.06±0.15	0.01±0.15
Adatom site	Unfaulted and faulted halves	
Δz_{A} (Å)	+0.04±0.20	
Δz_1 (Å)	-0.17±0.20	
$\Delta z_{2'}$ (Å)	-0.19±0.20	

TABLE III. Optimum values of the structural parameters determined by photoelectron diffraction for a reacted Si(111)(7×7) surface with the NH₂ fragments adsorbed atop of the silicon adatoms with the constraint that the local structure in the faulted and unfaulted halves of the surface unit mesh should be the same.

	Unfaulted and Faulted halves
d_{NA} (Å)	1.70±0.02
θ_{NA} (°)	0
z_{N1} (Å)	3.10±0.10
r_1 (Å)	2.05(+0.20/-0.40)
$z_{\text{N2}'}$ (Å)	4.42±0.08
z_{N3} (Å)	5.85 (+0.25/-0.15)

and the reduction of a factor of 10 in the relative vibrational amplitude of the nearest neighbor due to correlated vibrations is implausibly large.

A comparison of the adatom and rest atom adsorption sites thus very clearly favors the rest atom site. Applying reasonable constraints gives R -factor values for the adatom geometry which are larger than that of the rest atom site by several times the variance. Lower values can be obtained, but only by making unreasonable assumptions regarding the vibrational amplitudes, or by introducing extra structural variables with somewhat unreasonable relative values, but even these modifications failed to produce R -factor values as low as that achieved for the rest atom site.

IV. GENERAL DISCUSSION AND CONCLUSIONS

While the results of the analysis presented above show clearly that the adsorption geometry of the N atoms in the adsorbed species strongly favors the rest atom atop site over the adatom atop site, there remain two related questions. One is simply this: can we be sure that *only* the rest atom sites are occupied, or could there be a cooccupation of both rest atom and adatom sites? The second question concerns the nature of the NH_x adsorbed species, and in particular the possibility that there may be two coadsorbed species, NH and NH₂. In order to address the first of these questions, a simple calculation was conducted in which the experimental PhD spectra were compared with the two optimized calculated spectra for

TABLE IV. Optimum values of structural determined by photoelectron diffraction for a reacted Si(111)(7×7) surface with the NH₂ fragments adsorbed atop of the silicon adatoms with the local geometries of the two halves of the surface unit mesh unconstrained.

	Unfaulted half	Faulted half
d_{NA} (Å)	1.70±0.03	
θ_{NA} (°)	0	
z_{N1} (Å)	3.04±0.10	3.10±0.12
r_1 (Å)	2.05±0.30	2.05±0.30
$z_{\text{N2}'}$ (Å)	4.34±0.12	4.52±0.12
z_{N3} (Å)	5.87±0.10	6.12±0.10

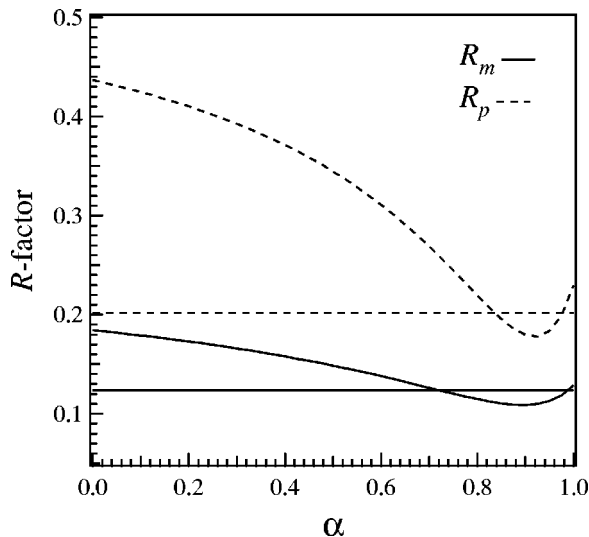


FIG. 7. Plot of the variation of the two R factors as a function of the relative occupation of the best-fit rest atom and adatom sites. All parameter values below the horizontal lines for the relevant R factor fall within the acceptable range of R -factor values.

the rest atom and adatom geometries in different relative amounts, i.e., the photoemitted intensity was assumed to take the form $I(k) = I_{\text{Rest}}(k)\alpha + I_{\text{Ad}}(k)(1 - \alpha)$. The variation of the two R factors with the parameter α is shown in Fig. 7. While this figure clearly shows that the rest atom geometry ($\alpha = 1$) gives R factors vastly superior to the pure adatom adsorption site ($\alpha = 0$), it also shows that a small addition of an adatom component leads to a reduction of the R factors which is just formally significant. The exact location of the minima in the two R factors differs slightly, as does the estimated precision, but a reasonable estimate of the value of α is 0.92 ± 0.07 ; i.e., an $8 \pm 7\%$ occupation of the adatom sites corresponds to the best fit structure. Strictly, we should optimize all the structural parameters of both models for all the values of α , as if there is a significant mixture of the two sites there is no reason why the geometry optimized on the assumption that only one site is occupied should be correct. However, it is clear that with such a modest fractional occupation of the adatom site, it is highly unlikely that such a more demanding optimization strategy would lead to significant differences in the resulting structures.

The problem of the possible existence of two coadsorbed molecular species is more difficult to resolve with complete confidence. It is well established that at sufficiently high temperatures adsorbed NH_2 may further dissociate to NH and ultimately N on $\text{Si}(111)$, but the relatively recent high-resolution core level photoemission study of Björkqvist *et al.*⁸ found evidence of two N-containing species at room temperature which, by comparison with HREELS evidence^{3,4} was interpreted as evidence of coadsorbed NH_2 and NH . The spectral resolution of our measurements was inadequate to identify these two components. We may, however, gain important information on this issue from our PhD results and, indeed, from our preferred estimate of the N surface coverage.

The main conclusion of our PhD study is that almost all

the N atoms are atop rest atoms. There are six such sites per 7×7 surface unit mesh, so a saturation of these sites alone by NH_2 would lead to a N coverage of $6/49 = 0.12$ ML, almost identical to the value of 0.13 ML which we obtained by the procedure we anticipate to be more reliable, namely, referring the N $1s$ emission intensity to that of the low energy Si L_{VV} Auger peak. Notice, too, that if NH_3 dissociation occurs by interaction with a rest atom/adatom pair, one might expect the saturation coverage to be determined by the (lower) number of rest atoms within the surface unit mesh. Of course, such a conclusion is independent of whether the NH_2 species occupies the rest atom or adatom sites, but nevertheless is specific to the surface NH_2 species alone.

We now consider the probable consequences of a significant coverage of coadsorbed NH on the PhD data. On the basis of conservation of bond order it is generally accepted in the literature that NH should bond to two Si surface atoms. If coadsorbed NH is present in twofold coordinated sites, the local N adsorption geometry will be of low symmetry relative to the surface point group, and the N atoms will not have a Si neighbor directly below the N atom. Indeed, inserting the NH between two surface Si atoms, as has been proposed, will also cause a distortion of the $\text{Si}(7 \times 7)$ surface which will lead to local disorder. The key consequence of these structural effects for photoelectron diffraction is that the PhD modulations arising from emission from these twofold coordinated NH species are expected to be weak (after averaging over symmetrically inequivalent directions) and, in particular, will be weak along the surface normal (with no favored Si backscattering geometry). Adding together the weakly modulated PhD spectra from these sites and from the more strongly modulated spectra from atop NH_2 species will therefore lead to an attenuation of the modulations arising from the atop species at near-normal emission (but no significant new structure). However, it is important to recognize that our methodology for analyzing experimental PhD modulation spectra involves matching not only the energetic locations of maxima and minima, but also the modulation amplitudes, and these are well matched by our existing calculations. Of course, as we have already remarked, the calculated modulation amplitudes are influenced by the vibrational amplitudes through a Debye-Waller factor. It would therefore be possible to enhance the calculated modulation amplitude to allow for some admixture of low-symmetry NH emission by reducing the vibrational amplitude. The key parameter determining the extent to which this would be possible is the relative mean square vibrational amplitude of the N emitter and the nearest-neighbor Si, as it is this scattering which dominates the PhD spectra. The value currently set (0.002 \AA^2) is, however, already quite low, being fractionally less than the absolute vibrational amplitudes expected for the bulk Si atoms, and thus already takes reasonable account of the expected correlation of the nearest-neighbor vibrations. Clearly, therefore, our results indicate that any co-occupation of low-symmetry sites by NH species must be low, almost certainly less than 20% of the total coverage of N-containing species, and more probably considerably less than this.

In summary, our results show that NH_2 on the $\text{Si}(111)$

$\times(7\times 7)$ is adsorbed (almost) exclusively atop Si surface rest atoms with a Si-N bond length of 1.71 ± 0.02 Å and very little modification of the geometry of the Si atoms in the layer below. We infer that the coadsorbed atomic hydrogen atoms are likely to be adsorbed atop the Si adatoms. Any coadsorbed NH on the surface, prepared by a reaction of NH₃ with Si(111)(7×7) at room temperature, is either of low relative coverage or is also adsorbed in local atop sites. There is evidence that a small fraction ($8\pm 7\%$) of the NH_x species may occupy sites atop Si surface adatoms.

ACKNOWLEDGMENTS

This work was supported by the German Federal Ministry of Education, Science, Research and Technology (Contract No. 05 625EBA 6), by the Engineering and Physical Science Research Council (UK), by a CSIC/CONICET collaboration project between Spain (under Grant No. MAT2002-03431) and Argentina, and by the European Union through a HCM Network (Grant No. ERBFMGMF CT 950031), and through the Large Scale Facilities program. The authors thank V. Fritzsche for providing the multiple scattering codes.

-
- ¹L. Kubler, E. K. Mil, D. Bolmont, and G. Gewinner, *Surf. Sci.* **183**, 503 (1987).
²S. Tanaka, M. Onchi, and M. Nishijima, *Surf. Sci.* **191**, L756 (1987).
³M. L. Colaianni, P. J. Chen, and J. T. Yates, *J. Chem. Phys.* **96**, 7826 (1992).
⁴P. J. Chen, M. L. Colaianni, and J. T. Yates, *Surf. Sci.* **274**, L605 (1992).
⁵F. Bozso and Ph Avouris, *Phys. Rev. B* **38**, 3937 (1988).
⁶J. L. Bischoff, F. Lutz, D. Bolmont, and L. Kubler, *Surf. Sci.* **251/252**, 170 (1991).
⁷G. Dufour, F. Rochet, H. Roulet, and F. Sirotti, *Surf. Sci.* **304**, 33 (1994).
⁸M. Bjrkqvist, M. Gthelid, T. M. Grehk, and U. O. Karlsson, *Phys. Rev. B* **57**, 2327 (1998).
⁹Ph. Avouris and R. Wolkov, *Phys. Rev. B* **39**, 5091 (1989).
¹⁰S. M. Cherif, J.-P. Lacharme, and C. A. Sebenne, *Surf. Sci.* **243**, 113 (1991).
¹¹N. Franco, J. Avila, M. E. Davila, M. C. Asensio, D. P. Woodruff, O. Schaff, V. Fernandez, K.-M. Schindler, V. Fritzsche, and A. M. Bradshaw, *Phys. Rev. Lett.* **79**, 673 (1997).
¹²N. Franco, J. Avila, M. E. Davila, M. C. Asensio, D. P. Woodruff, O. Schaff, V. Fernandez, K.-M. Schindler, V. Fritzsche, and A. M. Bradshaw, *J. Phys.: Condens. Matter* **9**, 8419 (1997).
¹³D. P. Woodruff and A. M. Bradshaw, *Rep. Prog. Phys.* **57**, 1029 (1994).
¹⁴S.-H. Lee and M.-H. Kang, *Phys. Rev. B* **58**, 4903 (1998).
¹⁵K. Takayanagi, Y. Tanishiro, M. Takahashi, and S. Takahashi, *J. Vac. Sci. Technol. A* **3**, 1502 (1985).
¹⁶X. Lin, X. Xu, N. Wang, Q. Zhang, and M. C. Lin, *Chem. Phys. Lett.* **355**, 365 (2002).
¹⁷K. Cho, E. Kaxiras, and J. D. Joannopoulos, *Phys. Rev. Lett.* **79**, 5078 (1997).
¹⁸H. Ezzehar, Ph. Sonnet, C. Minot, and L. Stauffer, *Surf. Sci.* **454-456**, 358 (2000).
¹⁹E. Dietz, W. Braun, A. M. Bradshaw and R. L. Johnson, *Nucl. Instrum. Methods Phys. Res. A* **239**, 359 (1985).
²⁰D. P. Woodruff, R. Davis, N. A. Booth, A. M. Bradshaw, C. J. Hirschmugl, K.-M. Schindler, O. Schaff, V. Fernandez, A. Theobald, Ph. Hofmann, and V. Fritzsche, *Surf. Sci.* **357/358**, 19 (1996).
²¹Ph. Hofmann and K.-M. Schindler, *Phys. Rev. B* **47**, 13941 (1993).
²²Ph. Hofmann, K.-M. Schindler, S. Bao, A. M. Bradshaw, and D. P. Woodruff, *Nature (London)* **368**, 131 (1994).
²³D. P. Woodruff, P. Baumgärtel, J. T. Hoefl, M. Kittel, and M. Polcik, *J. Phys.: Condens. Matter* **13**, 10625 (2001).
²⁴H. Ascolani, J. Avila, N. Franco, and M. C. Asensio, *Phys. Rev. Lett.* **8**, 2604 (1997).
²⁵S. Bengió, H. Ascolani, N. Franco, J. Avila, M. C. Asensio, E. Dudzik, I. T. McGovern, T. Giessel, R. Lindsay, A. M. Bradshaw, and D. P. Woodruff, *Phys. Rev. B* **66**, 195322 (2002).
²⁶V. Fritzsche, *Surf. Sci.* **213**, 648 (1989).
²⁷V. Fritzsche, *J. Phys.: Condens. Matter* **2**, 1413 (1990).
²⁸V. Fritzsche, *Surf. Sci.* **265**, 187 (1992).
²⁹R. Dippel, K.-U. Weiss, K.-M. Schindler, P. Gardner, V. Fritzsche, A. M. Bradshaw, M. C. Asensio, X. M. Hu, D. P. Woodruff, and A. R. González-Elipe, *Chem. Phys. Lett.* **199**, 625 (1992).
³⁰S. Bengió, M. Martin, J. Avila, M. C. Asensio, and H. Ascolani, *Phys. Rev. B* **65**, 205326 (2002).
³¹J. B. Pendry, *J. Phys. C* **12**, 937 (1980).
³²N. A. Booth, R. Davis, R. Toomes, D. P. Woodruff, C. Hirschmugl, K.-M. Schindler, O. Schaff, V. Fernandez, A. Theobald, Ph. Hofmann, R. Lindsay, T. Giessel, P. Baumgärtel, and A. M. Bradshaw, *Surf. Sci.* **387**, 152 (1997).
³³S. Y. Tong, H. Huang, C. M. Wei, W. E. Packard, F. K. Men, G. Glander, and M. B. Webb, *J. Vac. Sci. Technol. A* **6**, 615 (1988).